Letter

Spontaneous fractional Josephson current in parafermion junctions

Kishore Iyer,[1,2] Amulya Ratnakar,[3] Aabir Mukhopadyay,[3] Sumathi Rao,[2] and Sourin Das[3]
[1]*Aix Marseille Université, Université de Toulon, CNRS, CPT, Marseille, France*
[2]*International Centre for Theoretical Sciences, Tata Institute of Fundamental Research, Bengaluru 560089, India*
[3]*Department of Physics, Indian Institute of Science Education and Research (IISER) Kolkata, Mohanpur 741246, West Bengal, India*

(Received 28 August 2022; revised 17 January 2023; accepted 6 March 2023; published 30 March 2023)

We study a parafermion Josephson junction comprising a pair of counterpropagating edge modes of two quantum Hall systems, proximitized by an s-wave superconductor. We show that the difference between the lengths (which can be controlled by external gates) of the two counterpropagating chiral edges at the Josephson junction, can act as a source of spontaneous phase bias. For the Laughlin filling fractions, $\nu = 1/m, m \in 2\mathbb{Z}+1$, this leads to an electrical control of either Majorana ($m = 1$) or parafermion ($m \neq 1$) zero modes.

DOI: 10.1103/PhysRevB.107.L121408

Parafermions [1–8] are exotic generalizations of the Majorana modes [9–18] which may give rise to topological qudits with a better fault tolerance [19,20] than Majorana qubits. The essential property of these excitations that make them relevant for quantum computation is their behavior under exchange—they transform as non-Abelian anyons. Non-Abelian anyons are higher-dimensional representations of the braid group where exchanges are represented by unitary matrices. So exchanging parafermions or braiding them will rotate the quantum state in the Hilbert space of the degenerate ground state manifold. This nonlocal nature of operations generated by non-Abelian braiding gives rise to fault tolerance, making systems hosting non-Abelian anyons promising platforms for quantum information processing.

Majorana modes are the simplest examples of excitations with non-Abelian statistics. This has spearheaded the experimental search for Majorana modes across several platforms such as one-dimensional wires [21–32], fractional Josephson effect experiments [33–40], etc. There is a growing consensus in the community that there exists incontrovertible experimental evidence for Majoranas, despite some drawbacks of the evidence [41].

Experimental searches for parafermions, on the other hand, are still in their infancy. Even minimal proposals for the detection of parafermions involve a pair of fractional quantum Hall (FQH) edge states, i.e., even the simplest proposals involve strong electron interactions. There exist several proposals to engineer parafermions involving multiple or multilayer FQH states or fractional topological insulator states proximitized by superconductors (and/or ferromagnets) [5–7,34,42–44]. On the experimental side, there has been evidence of crossed Andreev reflection of fractionally charged edge states in a graphene FQH system [4,45] proximitized with a superconducting lead, and more recently in semiconductor integer quantum Hall (IQH) systems [46], which are precursors to being able to localize parafermions.

In this Letter, our main focus is to reexamine the fractional Josephson effect that occurs when the edges of quantum Hall states are sandwiched between two superconductors. Crucially, we allow for the two edges to have independent gate-tunable lengths L_1 and L_2. For the IQH system, where the edge states can be described by free electrons, and the spectrum of the Andreev bound states shows a 4π fractional Josephson effect, we find that the finite independent lengths give rise to a spontaneous Josephson current. Related results have been discussed in Ref. [47] in the context of anomalous quantum spin Hall systems. We further find that this consequence persists for $\nu = 1/m$ FQH states, leading to a $4m\pi$ spontaneous fractional Josephson current as a function of the difference in the lengths of the two edges.

The Majorana case. The junction between the two IQH edge states described in Fig. 1 allows for the realization of a helical edge state [48,49], which when proximitized by the superconductors leads to a topological phase with effective p-wave superconducting correlations [16]. The ballistic Josephson junction hence formed is expected to show a 4π periodic Josephson effect, provided that fermion parity is preserved [12]. Further, we will allow the counterpropagating edges in the ballistic region to have different lengths (L_1 and L_2), which may be realized by appropriate gating, as shown schematically in Fig. 1(b).

We can write the Hamiltonian for the IQH edges proximitized by superconductors and ferromagnets as $H = H_0 + H_I$, where

$$H_0 = -i\hbar v_F \int dx[\psi_R^\dagger(x)\partial_x\psi_R(x) + \psi_R(x)\partial_x\psi_R^\dagger(x)]$$
$$+ i\hbar v_F \int dx[\psi_L^\dagger(x)\partial_x\psi_L(x) + \psi_L(x)\partial_x\psi_L^\dagger(x)],$$
$$H_I = \int dx[\Delta(x)\psi_R\psi_L + M(x)\psi_R^\dagger\psi_L + \text{H.c.}], \tag{1}$$

where $\psi_{R/L}$ are right/left-moving chiral fermionic fields and v_F is the Fermi velocity of the electrons in these edges. The pairing amplitude $\Delta(x)$ and the backscattering strength $M(x)$ have a spatial profile, determined by the setup. The presence of superconducting correlations on a finite patch of the fermionic edges can be reduced to Andreev boundary conditions on the edges of the fermionic fields in the free

 ©2023 American Physical Society

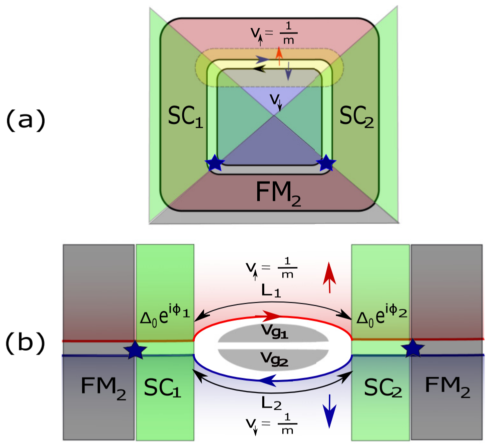

FIG. 1. (a) shows two concentric FQH liquids at filling fractions $\nu_{\uparrow/\downarrow} = 1/m$ ($m \in$ odd integer), colored red/blue, respectively, with counterpropagating edge modes and opposite spins. The edge modes are proximitized by two superconductors, SC_1 and SC_2, colored green, and a ferromagnet FM_2 colored gray. The encircled (yellow) region comprises the free edges and is magnified in (b). $V_{g_{1/2}}$ are gate potentials that can individually alter the length of the edges in the free region. $L_{1/2}$ are the lengths of the right-moving and left-moving edge modes, respectively. Δ_0 and ϕ_i are the superconducting gaps and the superconducting phases corresponding to SC_i. The two superconducting segments are considered to be the part of the same bulk superconductor. The blue stars at the interface between SC_i and FM_2 represent localized parafermion zero modes.

region of the setup [50–56] as shown below,

$$\psi_{R,\uparrow}(x=0) = e^{-i\Phi}e^{i\phi_1}\psi^\dagger_{L,\downarrow} \quad (x=0),$$
$$\psi_{R,\uparrow}(x=L_1) = e^{-i\Phi}e^{i\phi_2}\psi^\dagger_{L,\downarrow} \quad (x=L_2), \tag{2}$$

where $\Phi = \cos^{-1}(\frac{E}{\Delta_0})$, E is the Andreev bound state (ABS) energy, and ϕ_1 and ϕ_2 are the phases of the two superconducting regions. The boundary condition assumes that the superconductors are wide enough so that the Majorana modes localized at the interface between $SC_{1/2}$ and FM_2 do not influence it. The ABS spectrum can then be easily calculated to be [56,57]

$$E = \pm\Delta_0 \cos\left[\frac{E}{\Delta_0}\frac{\langle L\rangle}{L_{SC}} \pm \left(\frac{\mu\delta L}{\hbar v_F} - \frac{\phi}{2}\right)\right], \tag{3}$$

where μ denotes the Fermi energy, $\langle L\rangle = \frac{L_1+L_2}{2}$, $\delta L = \frac{L_1-L_2}{2}$, $\phi = \phi_1 - \phi_2$ is the difference of the two superconducting phases, and $L_{SC} = \hbar v_F/\Delta_0$ is the superconducting coherence length. The lengths L_1 and L_2 influence the ABS energy via the two independent linear combinations $\langle L\rangle$ and δL. Importantly, the term $\mu\delta L/\hbar v_F$ is additive with ϕ and hence has exactly the same effect as ϕ, i.e., $\delta L \neq 0$ leads to a spontaneous Josephson effect, even when $\phi = 0$. In the long junction limit, the ballistic region hosts multiple ABS, of which only one pair is topological, crossing $E = 0$ at $\theta = 2\mu\delta L/\hbar v_F - \phi = \pm\pi$. This can be confirmed by placing an impurity asymmetrically inside the junction [57]. Unlike the short junction limit [12,55,56,58] ($L_{1/2}/L_{SC} \longrightarrow 0$), where a single pair of topological ABS oscillates between the energy window $-\Delta_0$ to Δ_0, in the long junction limit, the energy window of the oscillation of topological ABS is shortened by the factor $L_{SC}/\langle L\rangle$.

Z_{2m} parafermions. Now we consider a setup where the two quantum Hall liquids at filling fractions $\nu = 1$ are replaced by $\nu = 1/m$ and this results in a $4m\pi$ Josephson effect [33–38,59]. As shown by Clarke *et al.* [7], this is one of the simplest theoretical proposals for realizing parafermion zero modes.

At the interface of the two quantum Hall liquids (shown in Fig. 1) the Hamiltonian for the gapless counterpropagating edge modes is given in bosonized form as

$$H_0 = \frac{mv_F}{4\pi}\int dx[(\partial_x\phi_R)^2 + (\partial_x\phi_L)^2]. \tag{4}$$

Here, v_F is the Fermi velocity and $m = 1/\nu$ is the inverse of the filling fraction and the chiral fields $\phi_{R,L}$ satisfy

$$[\phi_{R/L}(x), \phi_{R/L}(x')] = \pm i\frac{\pi}{m}\text{sgn}(x-x'),$$
$$[\phi_L(x), \phi_R(x')] = i\frac{\pi}{m}. \tag{5}$$

These properties are sufficient to ensure the proper anticommutation relations for the fermion operators defined as $\psi_{R/L} \sim e^{im\phi_{R/L}}$ [60–65].

Next, we briefly review the results of Lindner *et al.* [6] within our context. We imagine that the edge modes are fully gapped out by two alternating superconductors and ferromagnets [i.e., we imagine gapping out the free region in Fig. 1(a) by a ferromagnet FM_1]. The pairing due to the two superconductors and the insulating gap induced by electron backscattering are modeled by adding the appropriate cosine terms to the Hamiltonian, and the total Hamiltonian reads $H = H_0 + H_I$, where

$$H_I = \sum_{i=1,2}\left(\Delta_i\int_{SC_i} dx\cos\{m[\phi_R(x)+\phi_L(x)]\}\right.$$
$$\left.+\mathcal{M}_i\int_{FM_i} dx\cos\{m[\phi_R(x)-\phi_L(x)]\}\right). \tag{6}$$

The SC/FM proximitized regions are characterized by integer-valued charge/spin operators, called $\hat{Q}_j$ and $\hat{S}_j$, respectively. More precisely, since the charge is defined modulo $2e$ in the SC regions and the spin always changes in steps of 2 (due to backscattering) in the FM regions, the correct operators to describe the charge/spin in the SC/FM regions are $e^{i\pi\hat{Q}_j}$ and $e^{i\pi\hat{S}_j}$. These operators are related to the bosonic fields as

$$\hat{Q}_j = \int_{SC_j} dx\frac{1}{2\pi}\partial_x(\phi_R - \phi_L),$$
$$\hat{S}_j = \int_{FM_j} dx\frac{1}{2\pi}\partial_x(\phi_R + \phi_L). \tag{7}$$

In the limit where $\Delta_j, \mathcal{M}_j \longrightarrow \infty$, the $\phi_R \pm \phi_L$ fields in Eq. (6) are pinned to one of the $2m$ possible minima of the cosine, respectively. These minima are characterized by integer-valued operators $\hat{n}^{SC}_j$ in SC_j, and $\hat{n}^{FM}_j$ in FM_j. In the same limit, we can relate the operators $\hat{Q}_j, \hat{S}_j$ with $\hat{n}^{SC}_j, \hat{n}^{FM}_j$

using Eq. (7) giving us

$$\hat{Q}_j/\hat{S}_j = \frac{1}{m}\left(\hat{n}^{\mathrm{FM/SC}}_{j+1} - \hat{n}^{\mathrm{FM/SC}}_{j}\right), \tag{8}$$

where the index j is defined modulo 2. Note that the SC/FM regions can exchange $1/m$ charges/spins with the bulk of the FQH systems. This means that the operators $e^{i\pi\hat{Q}_j}$ and $e^{i\pi\hat{S}_j}$ can have eigenvalues $e^{i\pi q_j/m}$ and $e^{i\pi s_j/m}$, respectively, where $q_j, s_j \in \{0, 1, \dots, 2m-1\}$. We now define the total charge and spin operators, $\hat{Q}_{\mathrm{tot}}$, $\hat{S}_{\mathrm{tot}}$, which satisfy the global constraint $e^{i\pi\hat{Q}_{\mathrm{tot}}/\hat{S}_{\mathrm{tot}}} = \prod_j e^{i\pi\hat{Q}_j/\hat{S}_j} = e^{i\pi(n_\uparrow \pm n_\downarrow)/m}$, where $n_{\uparrow/\downarrow}$ are the number of quasiparticles in the spin up/down bulk FQH regions. For a general m, the number of distinct values of $\{n_\uparrow, n_\downarrow\}$ consistent with the global constraints is $(2m)^2/2$ [6]. Since the two superconducting (ferromagnetic) segments are considered to be parts of the same bulk superconductor (ferromagnet) (and the bulk SC is not assumed to be grounded), the total charge $q_{\mathrm{tot}} = q_1 + q_2$ and the total spin $s_{\mathrm{tot}} = s_1 + s_2$ of the system are conserved.

We hence label the ground state manifold by the eigenvalues of a *complete set of mutually commuting operators.* The commutation relations detailed in the Supplemental Material [57] show that our system hosts two such sets: $(e^{i\pi\hat{Q}_1}, e^{i\pi\hat{Q}_2}, \hat{S}_{\mathrm{tot}}, H)$ and $(e^{i\pi\hat{S}_1}, e^{i\pi\hat{S}_2}, \hat{Q}_{\mathrm{tot}}, H)$. The eigenvalues of both sets of operators provide an equivalent description of the ground state manifold of the system as long as the system is fully gapped by alternating superconductors and ferromagnets. The degeneracy can then be counted by the distinct set of eigenvalues of the operators in a particular basis subjected to global constraints. Note that for a fixed $\{n_\uparrow, n_\downarrow\}$ sector, s_1 and s_2 are not independent. The commutation relations outlined in the Supplemental Material show that if $|s_1, s_2, q_{\mathrm{tot}}\rangle$ is the eigenstate of the spin-parity operator $e^{i\pi\hat{S}_i}$, then so is $(e^{i\pi\hat{Q}_1})^k|s_1, s_2, q_{\mathrm{tot}}\rangle = |s_1 + k, s_2 - k, q_{\mathrm{tot}}\rangle$, where $k \in \{0, \dots, 2m-1\}$. Hence, the ground state manifold is $2m$-fold degenerate for a fixed $\{n_\uparrow, n_\downarrow\}$. Counting all possible values of $\{n_\uparrow, n_\downarrow\}$ gives the dimension of the ground state Hilbert space to be $(2m)^3/2$. The same set of arguments above can be repeated for the states labeled by $|q_1, q_2, s_{\mathrm{tot}}\rangle$ to obtain the same results.

Now, let us remove one of the insulating gaps by taking $\mathcal{M}_1 \to 0$. This leads to the realization of the ballistic Josephson junction setup as given in Fig. 1(a). For fixed $\{n_\uparrow, n_\downarrow\}$, the $2m$ states, which were degenerate ground states in the large $\mathcal{M}_1$ limit, now move away from zero energy and are no longer degenerate. The actual splitting of the energy depends on the various parameters ϕ, δL, and $\langle L\rangle$. Furthermore, as $\mathcal{M}_1 \to 0$, the charge parity operators $e^{i\pi\hat{Q}_i}$ no longer commute with the Hamiltonian, that is, $[e^{i\pi\hat{Q}_i}, H] \neq 0$. However, the other set of operators, $\hat{S}_1$, $\hat{S}_2$, and $\hat{Q}_{\mathrm{tot}}$, still commutes with the Hamiltonian. This means that rather than the basis, $|q_1, q_2, s_{\mathrm{tot}}\rangle$, we should use the eigenvalues of the set of mutually commuting operators $\hat{S}_1$, $\hat{S}_2$, $\hat{Q}_{\mathrm{tot}}$ to label the states as $|\bar{s}_1, \bar{s}_2, q_{tot}\rangle$. Note that we now label the eigenstates with the eigenvalues $\bar{s}_j$ of the operator $\hat{S}_j$ rather than those of the spin-parity $e^{i\pi\hat{S}_j}$ since removing FM_1 precludes backscattering between the edges. We will show later that the energy eigenvalue depends only on the spin in the ballistic Josephson junction region and is given by $H|\bar{s}_1, \bar{s}_2, q_{\mathrm{tot}}\rangle = E(\bar{s}_1)|\bar{s}_1, \bar{s}_2, q_{\mathrm{tot}}\rangle$ [see Eq. (14)]. Thus, the $2m$ ground states, which were degenerate at $E = 0$ in the $\mathcal{M}_1 \to \infty$ limit, are now at different energies $E(\bar{s}_1)$ for the $2m$ possible values of $\bar{s}_1$. As we change the phase factor $\theta = 2\mu\delta L/\hbar v_F - \phi$, the eigenvalues oscillate and cross each other.

As was shown earlier, the effective theory of the Josephson junction between SC_1 and SC_2, when $L_1 = L_2$, exhibits the Josephson effect with a periodicity $4\pi m$ [7]. For different lengths, we first note that the ABS spectrum derived in Ref. [57] essentially used the fact that particles and holes transform back into themselves after two consecutive Andreev reflections, having traversed a path of length $L_1 + L_2$. Thus, the spectrum includes the effect of the Andreev reflections as well as the dynamical phases. In terms of twisted boundary conditions, this translates to

$$\begin{aligned}\psi_R(x + L_1 + L_2) &= e^{-2i\Phi} e^{i(k_e L_1 - k_h L_2 + \phi_2 - \phi_1)}\psi_R(x)\\ &\equiv e^{i\sigma}\psi_R(x),\end{aligned} \tag{9}$$

where $\sigma/2 = -\cos^{-1}(\frac{E}{\Delta_0}) + \frac{E\langle L\rangle}{\hbar v_F} \pm (\frac{\mu\delta L}{\hbar v_F} - \frac{\phi}{2})$ represents all the phases accumulated by an electron when it traverses the loop defined by Andreev reflections between the two ends of the junction, and $\phi \equiv \phi_2 - \phi_1$. In terms of the bosonized Hamiltonian, this translates into the superconducting coupling between the two counterpropagating edge states of the following form,

$$\begin{aligned}H_{\mathrm{SC}} = -\Delta_0\bigg(&\int_{-l_{\mathrm{SC}}}^{0} dx \cos\{m[\phi_R(x) + \phi_L(x)]\}\\ &+ \int_{L_1}^{L_1 + l_{\mathrm{SC}}} dx \cos\{m[\phi_R(x) + \phi_L(x - 2\delta L)] + \sigma\}\bigg),\end{aligned} \tag{10}$$

where l_{SC} is the length of the superconducting regions. Note also that all the phases (σ) accumulated in traversing the loop between the two superconductors have been plugged into the second superconductor using gauge freedom. Δ_0 is the magnitude of the superconducting pairing.

Thus, the total Hamiltonian is given by $H = H_0 + H_{\mathrm{SC}}$. In the $\Delta_0 \longrightarrow \infty$ limit, the field $\phi_R + \phi_L$ is confined to the minima of the cosine potential and $E \ll \Delta_0$, giving us $\sigma = 2\pi \pm (\frac{2\mu\delta L}{\hbar v_F} - \phi)$, resulting in the following boundary conditions for the finite-length chiral Luttinger liquids in the junction between the two superconductors,

$$\begin{aligned}\phi_R(0) + \phi_L(0) &= 0,\\ \phi_R(L_1) + \phi_L(L_2) &= 2\Big(\mathrm{mod}\Big[\frac{\pi}{m}\Big(\hat{n}^{\mathrm{SC}}_2 - \frac{\sigma}{2\pi}\Big), 2\pi\Big] - \pi\Big)\\ &\equiv 2\hat{\eta},\end{aligned} \tag{11}$$

where $\hat{n}^{\mathrm{SC}}_2$ is an integer-valued operator corresponding to the pinned minimum of the fields at the right superconductor such that it can assume $2m$ values, $n^{\mathrm{SC}}_2 \in \{0, 2m-1\}$. $\hat{n}^{\mathrm{SC}}_1$ can be taken as zero without loss of generality. The modulus is necessary to ensure the compactness of the finite-length bosonic fields. It is interesting to note from Eq. (7) that $\hat{\eta}/\pi$ is nothing but the spin $\hat{S}_1$ of the junction.

The effective Hamiltonian for the ballistic junction between the two superconductors is given by

$$H_{\text{eff}} = \frac{mv_F}{4\pi} \int_{-L_2}^{L_1} dx(\partial_x \phi_R(x))^2, \tag{12}$$

where $\phi_R(x, t)$ is given by [8,57]

$$\begin{aligned}\phi_R(x) =& \frac{2\hat{\eta}}{L_1 + L_2}(x - L_1) + \hat{\chi} \\ &+ \frac{1}{\sqrt{m}} \sum_{k>0} \frac{1}{\sqrt{k}} \left(\hat{a}_k e^{\frac{2\pi ik}{L_1+L_2}(x-L_1)} + \hat{a}_k^\dagger e^{-\frac{2\pi ik}{L_1+L_2}(x-L_1)}\right),\end{aligned} \tag{13}$$

with $\phi_L(x) = -\phi_R(-x)$ and $[n_2^{\text{SC}}, \hat{\chi}] = i$, such that Eqs. (5) and (11) are satisfied. This diagonalizes the effective Hamiltonian, giving us

$$H_{\text{eff}} = \frac{mv_F}{\pi(L_1 + L_2)}\hat{\eta}^2 + \sum_{k>0} \frac{2\pi k v_F}{L_1 + L_2}\left(a_k^\dagger a_k + \frac{1}{2}\right). \tag{14}$$

In Eq. (14), the first term carries the dependence of energy on the SC phase difference ϕ and on the additional phase arising due to the length difference of the two chiral edges. Importantly, we note $[H_{\text{eff}}, \hat{n}_2^{\text{SC}}] = 0$, making $\hat{n}_2^{\text{SC}}$ a conserved quantity. For a fixed eigenvalue of the $\hat{n}_2^{\text{SC}}$ operator, the energy is $4m\pi$ periodic in $\theta = 2\mu\delta L/\hbar v_F - \phi$. The Josephson current across the ballistic region, $I_\theta \propto d\langle H_{\text{eff}}\rangle/d\theta$, also shows $4m\pi$ periodicity in θ and the characteristic *sawtooth* behavior. For $m = 1$ (Majorana modes), $\hat{n}_2^{\text{SC}}$ can be either 0 or 1, corresponding to even and odd fermion parity of the Josephson junction. Note that $\langle H_{\text{eff}}\rangle$ is a parity resolved expectation value. This specific case has been studied in detail earlier [66].

Discussion and conclusion. We show that allowing the length of the chiral edges of two quantum Hall systems (forming a Josephson junction) to be different leads to a spontaneous fractional Josephson effect. This introduces an experimental knob, on equal footing with the SC phase bias, that is far more amenable. We first demonstrated the feasibility in an IQH setup where the Andreev modes can be computed exactly.

Extending the bosonization scheme to address junctions of chiral Luttinger liquids with unequal lengths, we then study a $\nu = 1/m$ setup with Z_{2m} parafermions between the superconductors. This leads to a spontaneous $4\pi m$ Josephson effect tunable by the length difference of the chiral edges (δL). Such a finding may be of importance because it provides an extra handle on the Josephson current, controllable by electrical means, to probe parafermions. Our results are also valid for fractional topological insulators, where earlier work has already shown the existence of a $4m\pi$ Josephson effect [34]. Note that in changing δL, one also changes the area of the Josephson junction. The magnetic field required to host the quantum Hall effect changes the Aharanov-Bohm phase

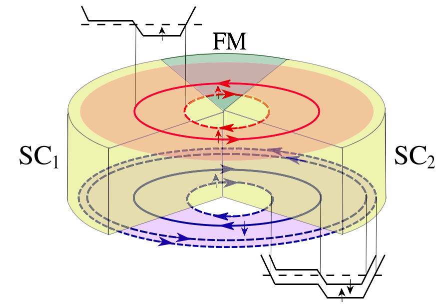

FIG. 2. A proposed setup to realize the fractional Josephson effect in a bilayer FQH system, with the top layer at $\nu = 1/m$ and the bottom layer at $\nu = 1 + 1/m$. The Landau levels are manipulated using appropriate gating such that two counterpropagating chiral states with opposite spins are brought together. The chiral states at the middle of the sample (shown in red and blue solid lines) are of importance to realize Josephson junction geometry. These chiral states are proximitized by two superconductors, SC$_1$ and SC$_2$, and a ferromagnet (FM) at the back. The length of the individual counterpropagating chiral states, in the ballistic region, can be altered using the external gates, which can drive the fractional Josephson current and show $4\pi m$ periodicity. Inconsequential chiral edge states are shown with dashed lines (red and blue) in the two layers.

experienced by the quasiparticles, adding to the Josephson phase. This phase can be calculated precisely in any geometry and excluded to isolate the effects of varying δL. For $v_F \sim 10^4$ m/s and $\mu \sim 10$ meV [67,68], the change in δL required to access the $4\pi m$ Josephson effect turns out to be a few μm in conventional two-dimensional electron gas (2DEG) systems, making it experimentally accessible by current standards.

To this end, we propose a setup to realize the spontaneous fractional Josephson current in a 2DEG embedded in a double quantum well tuned to two different FQH states (see Fig. 2). This setup is inspired by the experiment in Ref. [49]. We get two counterpropagating chiral edge states at the center of two FQH system with opposite spins, which can be proximitized by SC and FM as shown in Fig. 2. The external gates used to manipulate the Landau levels can also be used to displace the edges at the center of the sample and hence change the length of the chiral edges in the free region. This external control on the length of the chiral edges gives an experimental handle to realize the spontaneous fractional Josephson effect.

Acknowledgments. We acknowledge early collaboration with Krashna Mohan Tripathi and wish to thank him for many useful discussions. A.R. acknowledges University Grants Commission, India, for support in the form of a fellowship. S.D. would like to acknowledge the MATRICS grant (Grant No. MTR/ 2019/001 043) from the Science and Engineering Research Board (SERB) for funding. S.D. also acknowledges warm hospitality from ICTS during the final stages of writing the draft. K.I. thanks the ICTS - Long Term Visiting Students Program 2021.

K.I. and A.R. contributed equally to this work.

[1] P. Fendley, Parafermionic edge zero modes in Zn-invariant spin chains, J. Stat. Mech.: Theory Exp. (2012) P11020.

[2] L. Fidkowski and A. Kitaev, Topological phases of fermions in one dimension, Phys. Rev. B **83**, 075103 (2011).

[3] J. Alicea and P. Fendley, Topological phases with parafermions: Theory and blueprints, Annu. Rev. Condens. Matter Phys. **7**, 119 (2016).
[4] G.-H. Lee, K.-F. Huang, D. K. Efetov, D. S. Wei, S. Hart, T. Taniguchi, K. Watanabe, A. Yacoby, and P. Kim, Inducing superconducting correlation in quantum Hall edge states, Nat. Phys. **13**, 693 (2017).
[5] A. Vaezi, Fractional topological superconductor with fractionalized Majorana fermions, Phys. Rev. B **87**, 035132 (2013).
[6] N. H. Lindner, E. Berg, G. Refael, and A. Stern, Fractionalizing Majorana Fermions: Non-Abelian Statistics on the Edges of Abelian Quantum Hall States, Phys. Rev. X **2**, 041002 (2012).
[7] D. J. Clarke, J. Alicea, and K. Shtengel, Exotic non-Abelian anyons from conventional fractional quantum Hall states, Nat. Commun. **4**, 1348 (2013).
[8] U. Khanna, M. Goldstein, and Y. Gefen, Parafermions in a multilegged geometry: Towards a scalable parafermionic network, Phys. Rev. B **105**, L161101 (2022).
[9] A. Y. Kitaev, Unpaired Majorana fermions in quantum wires, Phys. Usp. **44**, 131 (2001).
[10] N. Read and D. Green, Paired states of fermions in two dimensions with breaking of parity and time-reversal symmetries and the fractional quantum Hall effect, Phys. Rev. B **61**, 10267 (2000).
[11] J. Nilsson, A. R. Akhmerov, and C. W. J. Beenakker, Splitting of a Cooper Pair by a Pair of Majorana Bound States, Phys. Rev. Lett. **101**, 120403 (2008).
[12] L. Fu and C. L. Kane, Josephson current and noise at a superconductor/quantum-spin-Hall-insulator/superconductor junction, Phys. Rev. B **79**, 161408(R) (2009).
[13] Y. Oreg, G. Refael, and F. von Oppen, Helical Liquids and Majorana Bound States in Quantum Wires, Phys. Rev. Lett. **105**, 177002 (2010).
[14] A. Das, Y. Ronen, Y. Most, Y. Oreg, M. Heiblum, and H. Shtrikman, Zero-bias peaks and splitting in an Al–Inas nanowire topological superconductor as a signature of Majorana fermions, Nat. Phys. **8**, 887 (2012).
[15] R. M. Lutchyn, J. D. Sau, and S. Das Sarma, Majorana Fermions and a Topological Phase Transition in Semiconductor-Superconductor Heterostructures, Phys. Rev. Lett. **105**, 077001 (2010).
[16] J. Alicea, New directions in the pursuit of Majorana fermions in solid state systems, Rep. Prog. Phys. **75**, 076501 (2012).
[17] S. D. Sarma, M. Freedman, and C. Nayak, Majorana zero modes and topological quantum computation, npj Quantum Inf. **1**, 15001 (2015).
[18] J. D. S. Bommer, H. Zhang, O. Gül, B. Nijholt, M. Wimmer, F. N. Rybakov, J. Garaud, D. Rodic, E. Babaev, M. Troyer, D. Car, S. R. Plissard, E. P. A. M. Bakkers, K. Watanabe, T. Taniguchi, and L. P. Kouwenhoven, Spin-Orbit Protection of Induced Superconductivity in Majorana Nanowires, Phys. Rev. Lett. **122**, 187702 (2019).
[19] M. Cheng, R. M. Lutchyn, and S. Das Sarma, Topological protection of Majorana qubits, Phys. Rev. B **85**, 165124 (2012).
[20] J. Preskill, Quantum computing and the entanglement frontier, arXiv:1203.5813.
[21] G. Ben-Shach, A. Haim, I. Appelbaum, Y. Oreg, A. Yacoby, and B. I. Halperin, Detecting Majorana modes in one-dimensional wires by charge sensing, Phys. Rev. B **91**, 045403 (2015).
[22] A. Cook and M. Franz, Majorana fermions in a topological-insulator nanowire proximity-coupled to an *s*-wave superconductor, Phys. Rev. B **84**, 201105(R) (2011).
[23] B. I. Halperin, Y. Oreg, A. Stern, G. Refael, J. Alicea, and F. von Oppen, Adiabatic manipulations of Majorana fermions in a three-dimensional network of quantum wires, Phys. Rev. B **85**, 144501 (2012).
[24] Y. Oreg, E. Sela, and A. Stern, Fractional helical liquids in quantum wires, Phys. Rev. B **89**, 115402 (2014).
[25] D. J. Clarke, J. D. Sau, and S. Tewari, Majorana fermion exchange in quasi-one-dimensional networks, Phys. Rev. B **84**, 035120 (2011).
[26] T. D. Stanescu and S. Tewari, Majorana fermions in semiconductor nanowires: Fundamentals, modeling, and experiment, J. Phys.: Condens. Matter **25**, 233201 (2013).
[27] L. Fidkowski, R. M. Lutchyn, C. Nayak, and M. P. A. Fisher, Majorana zero modes in one-dimensional quantum wires without long-ranged superconducting order, Phys. Rev. B **84**, 195436 (2011).
[28] M. Kjaergaard, K. Wölms, and K. Flensberg, Majorana fermions in superconducting nanowires without spin-orbit coupling, Phys. Rev. B **85**, 020503(R) (2012).
[29] E. Prada, P. San-Jose, M. W. de Moor, A. Geresdi, E. J. Lee, J. Klinovaja, D. Loss, J. Nygård, R. Aguado, and L. P. Kouwenhoven, From Andreev to Majorana bound states in hybrid superconductor–semiconductor nanowires, Nat. Rev. Phys. **2**, 575 (2020).
[30] F. Setiawan, W. S. Cole, J. D. Sau, and S. Das Sarma, Transport in superconductor–normal metal–superconductor tunneling structures: Spinful *p*-wave and spin-orbit-coupled topological wires, Phys. Rev. B **95**, 174515 (2017).
[31] F. Setiawan, W. S. Cole, J. D. Sau, and S. Das Sarma, Conductance spectroscopy of nontopological-topological superconductor junctions, Phys. Rev. B **95**, 020501(R) (2017).
[32] J. D. Sau and F. Setiawan, Detecting topological superconductivity using low-frequency doubled Shapiro steps, Phys. Rev. B **95**, 060501(R) (2017).
[33] M. Cheng and R. Lutchyn, Fractional Josephson effect in number-conserving systems, Phys. Rev. B **92**, 134516 (2015).
[34] M. Cheng, Superconducting proximity effect on the edge of fractional topological insulators, Phys. Rev. B **86**, 195126 (2012).
[35] L. Jiang, D. Pekker, J. Alicea, G. Refael, Y. Oreg, and F. von Oppen, Unconventional Josephson Signatures of Majorana Bound States, Phys. Rev. Lett. **107**, 236401 (2011).
[36] C.-K. Chiu and S. Das Sarma, Fractional Josephson effect with and without Majorana zero modes, Phys. Rev. B **99**, 035312 (2019).
[37] S. Frolov, M. Manfra, and J. Sau, Topological superconductivity in hybrid devices, Nat. Phys. **16**, 718 (2020).
[38] L. P. Rokhinson, X. Liu, and J. K. Furdyna, The fractional ac Josephson effect in a semiconductor–superconductor nanowire as a signature of Majorana particles, Nat. Phys. **8**, 795 (2012).
[39] I. V. Bobkova, A. M. Bobkov, A. A. Zyuzin, and M. Alidoust, Magnetoelectrics in disordered topological insulator Josephson junctions, Phys. Rev. B **94**, 134506 (2016).
[40] M. Alidoust and H. Hamzehpour, Spontaneous supercurrent and φ_0 phase shift parallel to magnetized topological insulator interfaces, Phys. Rev. B **96**, 165422 (2017).

[41] D. Castelvecchi, Evidence of elusive Majorana particle dies with retraction, Nature (London) **591**, 354 (2021).

[42] R. S. K. Mong, D. J. Clarke, J. Alicea, N. H. Lindner, P. Fendley, C. Nayak, Y. Oreg, A. Stern, E. Berg, K. Shtengel, and M. P. A. Fisher, Universal Topological Quantum Computation from a Superconductor-Abelian Quantum Hall Heterostructure, Phys. Rev. X **4**, 011036 (2014).

[43] M. Barkeshli and X.-L. Qi, Synthetic Topological Qubits in Conventional Bilayer Quantum Hall Systems, Phys. Rev. X **4**, 041035 (2014).

[44] N. Schiller, E. Cornfeld, E. Berg, and Y. Oreg, Predicted signatures of topological superconductivity and parafermion zero modes in fractional quantum Hall edges, Phys. Rev. Res. **2**, 023296 (2020).

[45] O. Gül, Y. Ronen, S. Y. Lee, H. Shapourian, J. Zauberman, Y. H. Lee, K. Watanabe, T. Taniguchi, A. Vishwanath, A. Yacoby, and P. Kim, Andreev Reflection in the Fractional Quantum Hall State, Phys. Rev. X **12**, 021057 (2022).

[46] M. Hatefipour, J. J. Cuozzo, J. Kanter, W. M. Strickland, C. R. Allemang, T.-M. Lu, E. Rossi, and J. Shabani, Induced superconducting pairing in integer quantum Hall edge states, Nano Lett. **22**, 6173 (2022).

[47] K. Sakurai, S. Ikegaya, and Y. Asano, Tunable-φ Josephson junction with a quantum anomalous Hall insulator, Phys. Rev. B **96**, 224514 (2017).

[48] J. D. Sanchez-Yamagishi, J. Y. Luo, A. F. Young, B. M. Hunt, K. Watanabe, T. Taniguchi, R. C. Ashoori, and P. Jarillo-Herrero, Helical edge states and fractional quantum Hall effect in a graphene electron–hole bilayer, Nat. Nanotechnol. **12**, 118 (2017).

[49] Y. Ronen, Y. Cohen, D. Banitt, M. Heiblum, and V. Umansky, Robust integer and fractional helical modes in the quantum Hall effect, Nat. Phys. **14**, 411 (2018).

[50] D. L. Maslov, M. Stone, P. M. Goldbart, and D. Loss, Josephson current and proximity effect in Luttinger liquids, Phys. Rev. B **53**, 1548 (1996).

[51] M. Stone and Y. Lin, Josephson currents in quantum Hall devices, Phys. Rev. B **83**, 224501 (2011).

[52] F. Crépin, B. Trauzettel, and F. Dolcini, Signatures of Majorana bound states in transport properties of hybrid structures based on helical liquids, Phys. Rev. B **89**, 205115 (2014).

[53] F. c. Crépin and B. Trauzettel, Parity Measurement in Topological Josephson Junctions, Phys. Rev. Lett. **112**, 077002 (2014).

[54] Y. Tanaka, T. Hirai, K. Kusakabe, and S. Kashiwaya, Theory of the Josephson effect in a superconductor/one-dimensional electron gas/superconductor junction, Phys. Rev. B **60**, 6308 (1999).

[55] A. Mukhopadhyay and S. Das, Thermal signature of the Majorana fermion in a Josephson junction, Phys. Rev. B **103**, 144502 (2021).

[56] A. Kundu, S. Rao, and A. Saha, Resonant tunneling through superconducting double barrier structures in graphene, Phys. Rev. B **82**, 155441 (2010).

[57] See Supplemental Material at http://link.aps.org/supplemental/10.1103/PhysRevB.107.L121408 for details on Andreev bound states and bosonization.

[58] H.-J. Kwon, V. Yakovenko, and K. Sengupta, Fractional ac Josephson effect in unconventional superconductors, Low Temp. Phys. **30**, 613 (2004).

[59] D. M. Badiane, L. I. Glazman, M. Houzet, and J. S. Meyer, ac Josephson effect in topological Josephson junctions, C. R. Phys. **14**, 840 (2013).

[60] F. Haldane, "Luttinger liquid theory" of one-dimensional quantum fluids. I. Properties of the Luttinger model and their extension to the general 1D interacting spinless Fermi gas, J. Phys. C **14**, 2585 (1981).

[61] S. Rao, *Field Theories in Condensed Matter Physics* (CRC Press, Boca Raton, FL, 2002).

[62] J. von Delft and H. Schoeller, Bosonization for beginners—refermionization for experts, Ann. Phys. **510**, 225 (1998).

[63] T. Giamarchi, *Quantum Physics in One Dimension*, Vol. 121 (Clarendon Press, Oxford, U.K., 2003).

[64] C. L. Kane and M. P. A. Fisher, Transport in a One-Channel Luttinger Liquid, Phys. Rev. Lett. **68**, 1220 (1992).

[65] While, for a single species of bosons, our convention where the left- and right-moving bosons have nontrivial commutation relations is sufficient to take care of Fermi statistics, the introduction of more species will require Klein factors to ensure correct Fermi statistics between fermion operators.

[66] C. W. J. Beenakker, D. I. Pikulin, T. Hyart, H. Schomerus, and J. P. Dahlhaus, Fermion-Parity Anomaly of the Critical Supercurrent in the Quantum Spin-Hall Effect, Phys. Rev. Lett. **110**, 017003 (2013).

[67] Z.-X. Hu, E. H. Rezayi, X. Wan, and K. Yang, Edge-mode velocities and thermal coherence of quantum Hall interferometers, Phys. Rev. B **80**, 235330 (2009).

[68] E. P. De Poortere, Y. P. Shkolnikov, E. Tutuc, S. J. Papadakis, M. Shayegan, E. Palm, and T. Murphy, Enhanced electron mobility and high order fractional quantum Hall states in AlAs quantum wells, Appl. Phys. Lett. **80**, 1583 (2002).